Predefined-Time Guaranteed Performance Attitude Tracking Control of Flexible Spacecraft Based on Multi-observers

DENG Xingting^{1,2}, ZHANG Ziyang¹, WANG Beichao¹, WANG Guohua², LI Fangfang², LI Shuang^{1*}

College of Astronautics, Nanjing University of Aeronautics and Astronautics, Nanjing 211106, P. R. China;
 Shanghai Engineering Center for Microsatellites, Shanghai 201306, P. R. China

(Received 8 June 2025; revised 23 July 2025; accepted 14 August 2025)

Abstract: To overcome external environmental disturbances, inertial parameter uncertainties and vibration of flexible modes in the process of attitude tracking, a comprehensively effective predefined-time guaranteed performance controller based on multi-observers for flexible spacecraft is proposed. First, to prevent unwinding phenomenon in attitude description, the rotation matrix is used to represent the spacecraft's attitude. Second, the flexible modes observer which can guarantee predefined-time convergence is designed, for the case where flexible vibrations are unmeasurable in practice. What's more, the disturbance observer is applied to estimate and compensate the lumped disturbances to improve the robustness of attitude control. A predefined-time controller is proposed to satisfy the prescribed performance and stabilize the attitude tracking system via barrier Lyapunov function. Finally, through comparative numerical simulations, the proposed controller can achieve high-precision convergence compared with the existing finite-time attitude tracking controller. This paper provides certain references for the high-precision predefined-time prescribed performance attitude tracking of flexible spacecraft with multi-disturbance.

Key words: flexible spacecraft; guaranteed performance; predefined-time control; multi-observers **CLC number:** V412.4 **Document code:** A **Article ID:** 1005-1120(2025)S-0026-12

0 Introduction

Spacecraft attitude control is of great significance to the success of space missions, which should possess high accuracy, stability, and robustness to meet the challenges of space environments and diverse mission requirements. In spacecraft's attitude tracking control systems, actuators' outputs are adjusted by the control algorithms to minimize the attitude errors relative to the desired attitude. However, influenced by multiple factors including unknown inertial parameters, complex environmental disturbances, and the elastic and rigid coupling effects, the actual attitude kinematics and dynamics of spacecraft are complex, leading to frequent challenges in attitude tracking process. Thus, a compre-

hensively effective controller for spacecraft attitude tracking control is essential. Recently, many methods have been proposed to handle these challenges, including robust control, adaptive disturbance rejection control, and disturbance observer-based control.

To improve the system's anti-disturbance capabilities, the adaptive control approaches that integrate sliding mode control and backstepping method are used for spacecraft's attitude control system, which is considered to have extensive conservation for the assumption that disturbances meet specific inequality constraints^[1-3]. What's more, since the neural network has the ability of online learning, which can update and adjust parameters to compensate for the lumped disturbances with estimation, thus it can avoid making priori assumptions^[4-5]. However, the

How to cite this article: DENG Xingting, ZHANG Ziyang, WANG Beichao, et al. Predefined-time guaranteed performance attitude tracking control of flexible spacecraft based on multi-observers [J]. Transactions of Nanjing University of Aeronautics and Astronautics, 2025, 42(S): 26-37.

^{*}Corresponding author, E-mail address: lishuang@nuaa.edu.cn.

disturbance suppression methods based on neural network involve a complex parameter tuning process, which may increase the computational burden and the time consumption of the control system. In this case, the disturbance observer-based control only requires selecting a few appropriate observer's gains to estimate the lumped disturbances in the system.

It can be seen that although these controllers have satisfactory robustness to the uncertainty of external disturbances and inherent moments of inertia, in the design of many of them, full state feedback is used. However, in practical applications, it is impossible to measure certain states of the system. The practical spacecraft attitude model is usually affected by flexible structures, such as solar cells and antennas, leading to a typical rigid-flexible coupling characteristic. This coupling effect will increase the difficulty of maintaining attitude control accuracy. What's more, modal variables are usually unmeasurable in flexible spacecraft. In recent years, using some special materials, such as piezoelectric materials, has been investigated by researchers as active vibration control strategies^[6]. However, piezoelectric sensors and actuators change the structure and properties of the flexible appendage due to mechanical interference, which is not permitted by most flexible constructions. Therefore, using piezoelectric sensors to measure modal variables of flexible spacecraft is not recommended for practical cases.

In addition, studies^[7-9] are modeled based on quaternions in describing a specific attitude, which may lead to an unwinding phenomenon, meaning the spacecraft may ignore one of the two equilibrium points of quaternions during the attitude maneuver, then it needs to rotate an angle more than 180° to reach the steady states, thus increasing unnecessary fuel consumption. It is shown by Ref.[10] which introduces a novel attitude error function based on the rotation matrix and then proposes a controller to realize attitude tracking of rigid spacecraft, thus it can essentially avoid the phenomenon of unwinding.

On another aspect, most space missions (such as docking and rendezvous of satellites) require to stabilize quickly. Although the finite-time theory^[11-12] can overcome the infinite convergence prob-

lem, the convergence time varies with different initial conditions, which cannot be determined in practice since the initial states are not exactly known. Fixed-time control, as special finite-time control, further guarantees that the upper bound of convergence time is independent of the initial conditions and related to the designed parameters^[13]. In this case, the predefined time control (PTC) theory is developed, the notable benefit of which is that the system's maximum convergence time can be explicitly represented by control parameters to make it a hotspot in the past few years^[14-17]. The predefinedtime controller proposed in Ref.[14] proposes a novel adaptive nonsingular predefined-time controller with backstepping recursive design method, and a quadratic function is designed to avoid singularities. Moreover, the authors in Ref.[17] propose two predefined-time sliding-mode observers to estimate the desired attitude and angular velocity in the case of only a set of spacecraft has access to them, and the proposed controller can achieve predefinedtime attitude tracking of a multi-spacecraft system.

The above studies share a common characteristic that focuses only on the steady-state behavior and do not consider the transient responses. In practice, ensuring ideal transient performance of attitude and angular velocity in the tracking process can be challenging. The well-known prescribed performance control (PPC) method has the capability to guarantee the system's transient performance (convergence speeds and overshoots) and steady-state performance (steady-state errors), which can meet the control requirements of practical tasks^[18-20]. The upper and lower bounds of the system states are referred as the prescribed performance functions, which introduce additional nonlinear constraints to the system, therefore increasing the complexity of controller design. It is necessary to map the system states into an unconstrained space using the transformation function, which leads to a complex structure of the system. What's more, the tracking errors can only be driven to a specified residual set as time approaches infinity with traditional performance functions.

Inspired by the mentioned studies, this paper

designs an attitude tracking controller based on the PPC method and PTC theory for flexible spacecraft under environmental disturbances, considering the inertial parameter uncertainties. The principal contributions of this study are concisely outlined as follows:

- (1) The advantages of the proposed observers are: The convergence time of the estimation errors can be explicitly represented in the observers; the disturbance observer does not require any priori information.
- (2) The upper bound of the convergence time of the system states can be arbitrarily predefined by setting the control parameters, which is independent from the system initial conditions.
- (3) The combination of finite-time prescribed performance functions and barrier Lyapunov functions (BLF) avoids introducing transformation functions to simplify controller design, which makes it more valuable in practical applications.

The rest of the paper is organized as follows: Flexible spacecraft attitude tracking error model based on the rotation matrix description is developed and the related lemmas are introduced in Section 1. The flexible mode observer and disturbance observer are designed in Section 2, followed by the controller design and stability proofs in Section 3. The numerical simulations are provided in Section 4, which can validate the effectiveness of the proposed algorithm. The conclusion is given in Section 5.

1 Spacecraft Modeling and Problem Formulation

1.1 Model of flexible spacecraft

To avoid unwinding phenomena during the attitude description, the attitude equation of the space-craft based on the rotation matrix is defined as follows

$$\dot{R} = R \omega^{\times} \tag{1}$$

where $R \in \mathbb{R}^{3\times3}$ is the rotation matrix that transforms the spacecraft from the body-fixed frame to the inertial frame.

In Figs.1,2, $O_i x_i y_i z_i$, $O_b x_b y_b z_b$, $O_a x_a y_a z_a$ and $O_d x_d y_d z_d$ represent the inertial frame, the body-fixed frame, the appendage frame, and the reference frame, respectively. Considering facts such as external environmental disturbances, inertial matrix uncertainties, actuator failures, and input saturation, the attitude dynamics of the flexible spacecraft based on the hybrid coordinate method can be derived using Lagrange's equations as follows

$$\begin{cases} J\dot{\boldsymbol{\omega}} + \boldsymbol{\delta}^{\mathrm{T}}\boldsymbol{\eta} = -\boldsymbol{\omega}^{\times}(J\boldsymbol{\omega} + \boldsymbol{\delta}^{\mathrm{T}}\boldsymbol{\eta}) + \boldsymbol{u} + \boldsymbol{d} \\ \ddot{\boldsymbol{\eta}} + C\dot{\boldsymbol{\eta}} + K\boldsymbol{\eta} = -\boldsymbol{\delta}\dot{\boldsymbol{\omega}} \end{cases}$$
(2)

where $J = J_0 + \Delta J \in \mathbb{R}^{3 \times 3}$ is the actual inertia matrix of the spacecraft, containing $J_0 \in \mathbb{R}^{3 \times 3}$ as the nominal component and $\Delta J \in \mathbb{R}^{3 \times 3}$ as the uncertain part; $\delta \in \mathbb{R}^{n \times 3}$ represents the coupling matrix between rigid body and flexible structures of the spacecraft; $C = \text{diag} \{ [2\xi_1 l_1, 2\xi_2 l_2, \cdots, 2\xi_n l_n] \} \in \mathbb{R}^{n \times n}$; $K = \text{diag} \{ [l_1^2, l_2^2, \cdots, l_n^2] \} \in \mathbb{R}^{n \times n}$ denotes the damping

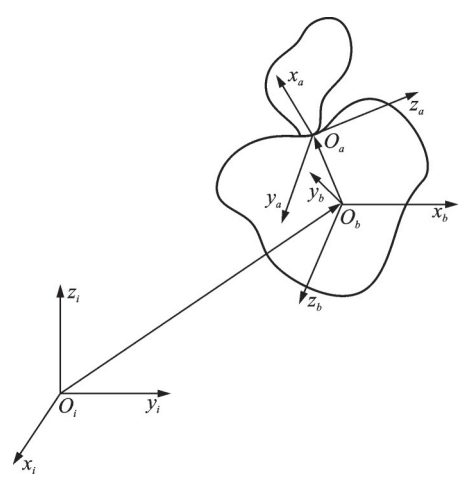


Fig.1 Spacecraft structure with a central rigid body and a flexible attachment

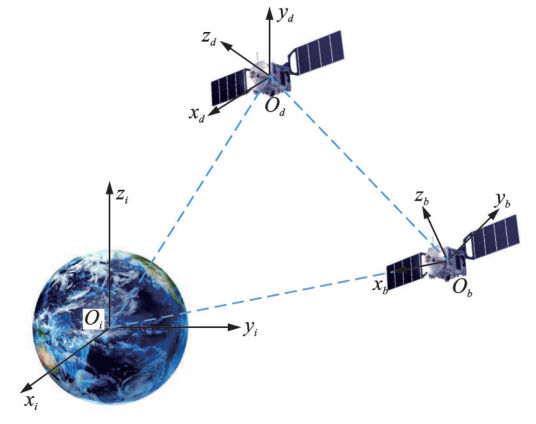


Fig.2 Spacecraft coordinate systems

matrix and the stiffness matrix, where ξ_i , l_i ($i = 1, 2, \dots, n$) are damping ratios and natural frequencies, respectively; $\eta \in \mathbb{R}^{n \times 1}$ denotes the flexible modes and n is the modal order; $d \in \eta \in \mathbb{R}^{n \times 13 \times 1}$ represents the environmental disturbance torque; $\boldsymbol{\omega} = [\boldsymbol{\omega}_1, \boldsymbol{\omega}_2, \boldsymbol{\omega}_3]^T \in \mathbb{R}^{3 \times 1}$ is the angular velocity of spacecraft in the body-fixed frame, and $\boldsymbol{\omega}^{\times}$ is given by

$$\boldsymbol{\omega}^{\times} = \begin{bmatrix} 0 & -\boldsymbol{\omega}_{3} & \boldsymbol{\omega}_{2} \\ \boldsymbol{\omega}_{3} & 0 & -\boldsymbol{\omega}_{1} \\ -\boldsymbol{\omega}_{z} & \boldsymbol{\omega}_{1} & 0 \end{bmatrix}$$
(3)

The attitude errors and angular velocity errors of the spacecraft are defined, respectively, as shown

$$\tilde{R} = R_{\rm d}^{\rm T} R \tag{4}$$

$$\tilde{\boldsymbol{\omega}} = \boldsymbol{\omega} - \tilde{R}^{\mathrm{T}} \boldsymbol{\omega}_{\mathrm{d}} \tag{5}$$

where $R_d \in R^{3 \times 3}$ and $\omega_d \in R^{3 \times 1}$ denote the desired rotation matrix and the desired angular velocity, respectively. The challenge in designing the attitude controller using the above model comes mainly from the complexity of the rotation matrix, which makes it more difficult to derive the controller directly. Therefore, an equivalent error model based on rotation matrix is introduced referring to Ref.[10].

$$\psi(\tilde{R}) = 2 - \sqrt{1 + \operatorname{tr}(\tilde{R})} \tag{6}$$

$$\boldsymbol{e}_{\tilde{\boldsymbol{R}}} = \frac{1}{2\sqrt{1 + \operatorname{tr}(\tilde{\boldsymbol{R}})}} \left(\tilde{\boldsymbol{R}} - \tilde{\boldsymbol{R}}^{\mathrm{T}} \right)^{\mathrm{V}} \tag{7}$$

where $\psi(\tilde{R})$ is the attitude error function and $e_{\tilde{R}} \in \mathbb{R}^3$ the transformed error vector. "V" denotes the inverse operation of " \times ", which can convert the skew-symmetric matrix into a three-dimensional vector: $SO(3) \rightarrow \mathbb{R}^3$. Based on Eqs.(1, 2) and Eqs.(6,7), the attitude tracking error dynamics of the spacecraft is derived as

$$\dot{\boldsymbol{e}}_{\tilde{n}} = E\tilde{\boldsymbol{\omega}} \tag{8}$$

$$\begin{cases} J\dot{\tilde{\omega}} = F + G + u \\ \ddot{\eta} + C\dot{\eta} + K\eta = -\delta\dot{\omega} \end{cases}$$
(9)

$$E = \frac{1}{2\sqrt{1 + \operatorname{tr}(\tilde{R})}} \left(\operatorname{tr}(\tilde{R}) I - \tilde{R}^{\mathrm{T}} + 2e_{\tilde{R}}e_{\tilde{R}}^{\mathrm{T}} \right) \quad (10)$$

$$F = -(\tilde{\boldsymbol{\omega}} + \tilde{R}^{\mathrm{T}} \boldsymbol{\omega}_{\mathrm{d}})^{\times} J(\tilde{\boldsymbol{\omega}} + \tilde{R}^{\mathrm{T}} \boldsymbol{\omega}_{\mathrm{d}}) - J \tilde{R}^{\mathrm{T}} \dot{\boldsymbol{\omega}}_{\mathrm{d}} + J \tilde{\boldsymbol{\omega}}^{\times} \tilde{R}^{\mathrm{T}} \boldsymbol{\omega}_{\mathrm{d}}$$

$$(11)$$

$$G = \tilde{\boldsymbol{\omega}}^{\times} \boldsymbol{\delta}^{\mathrm{T}} \dot{\boldsymbol{\eta}} - (\tilde{R}^{\mathrm{T}} \dot{\boldsymbol{\omega}}_{d})^{\times} \boldsymbol{\delta}^{\mathrm{T}} \dot{\boldsymbol{\eta}} - \boldsymbol{\delta}^{\mathrm{T}} \dot{\boldsymbol{\eta}} + d$$
 (12)

1. 2 Preliminary

Lemma 1^[21] For the system $\dot{x} = f(x)$,

x(0) = 0; for $x \in \mathbb{R}^n$ and $f: \mathbb{R}^n \to \mathbb{R}^n$, if a continuous positive-definite Lyapunov function V(x) satisfies the following inequality

$$\dot{V}(x) \leq -\frac{\pi}{pT_1\sqrt{\lambda_1\lambda_2}} \left[\lambda_1 V^{1-\frac{\rho}{2}}(x) + \lambda_2 V^{1+\frac{\rho}{2}}(x)\right] + \rho$$
(13)

where λ_1 , λ_2 , $T_c > 0$, $0 , <math>0 < \rho < \infty$, then the equilibrium point is practically predefined-time stable. If there exists $0 < \theta < 1$, the state of the system can converge within the predefined-time $T = \frac{1}{\sqrt{\theta}} T_c$, and the residual set of the solution in system is given by

$$\lim_{n \to \infty} x \in \{x \in \mathbf{R}^n | V(x) \leqslant \min \{D_1, D_2\}\}$$

where
$$D_1 = \left(\frac{\rho p T_c \sqrt{\lambda_1 \lambda_2}}{\pi \lambda_1 (1-\theta)}\right)^{\frac{2}{2-\rho}}, D_2 = \left(\frac{\rho p T_c \sqrt{\lambda_1 \lambda_2}}{\pi \lambda_2 (1-\theta)}\right)^{\frac{2}{2+\rho}}$$
.

Lemma 2^[22] For any arbitrary constants $x_i > 0$, $i = 1, 2, \dots, n$ and q > 0, the following inequalities holds

$$\begin{cases} \sum_{i=1}^{n} x_i^q \geqslant \left(\sum_{i=1}^{n} x_i\right)^q & 0 < q < 1 \\ \sum_{i=1}^{n} x_i^q \geqslant n^{1-q} \left(\sum_{i=1}^{n} x_i\right)^q & q > 1 \end{cases}$$

Lemma 1 is the predefined-time stability theory, which is developed based on the Lyapunov direct method. Lyapunov functions related to the system states can be constructed empirically, and the controller is designed using the backstepping method to satisfy Eq.(13). In this case, the system states convergence in predefined time.

Lemma 2 is typically employed in stability proofs for the constructed Lyapunov functions to satisfy Eq.(13).

2 Predefined-Time Observer

2. 1 Predefined-time flexible mode observer

To cope with problem of the unmeasurable flexible modes in practical situations, a predefined-time observer is designed for estimating the modes, and the convergence time of the estimation errors can be explicitly represented in the observer.

Denote $\phi = \dot{\eta} + \delta \omega$, and $\dot{\phi} = -(C\psi + K\eta - C\delta \omega)$, the second equation in Eq.(9) can be rewrit-

ten as

$$\dot{\chi} = \bar{A}\chi + \bar{B}\omega \tag{14}$$

where

$$\chi = \begin{bmatrix} \eta \\ \phi \end{bmatrix}, \bar{A} = \begin{bmatrix} 0 & I_{n \times n} \\ -K & -C \end{bmatrix}, \bar{B} = \begin{bmatrix} -\delta \\ C\delta \end{bmatrix}$$
The form of the predefined-time observer is

$$\dot{\hat{\chi}} = \bar{A}\hat{\chi} + \bar{B}\boldsymbol{\omega} - \left(\frac{\pi}{2p_1T_1}\left(\operatorname{sig}^{1-p_1}(\boldsymbol{\chi} - \hat{\boldsymbol{\chi}}) + 3^{\frac{p_1}{2}}\operatorname{sig}^{1+p_1}(\boldsymbol{\chi} - \hat{\boldsymbol{\chi}})\right) + \bar{A}(\boldsymbol{\chi} - \hat{\boldsymbol{\chi}}) - a\operatorname{sign}(\boldsymbol{\chi} - \hat{\boldsymbol{\chi}})\right)$$
(15)

where $\hat{\chi} = \begin{bmatrix} \hat{\eta} & \hat{\phi} \end{bmatrix}^T$, $0 < p_1 < 1$, a > 0, and $T_1 > 0$ is the upper bound on the convergence time of the estimation errors, which can be predefined. Denote the estimation errors as $\tilde{\chi} = \chi - \hat{\chi}$, the predefined time convergence of the proposed observer (Eq.(16))

can be proved by defining the Lyapunov candidate function as follows

$$V_{\mathbf{x}} = \frac{1}{2} \,\tilde{\mathbf{\chi}}^{\mathrm{T}} \tilde{\mathbf{\chi}} \tag{16}$$

The derivative of V_{χ} can be obtained as follows

$$\dot{V}_{\chi} = \tilde{\chi}^{T} \left(\dot{\chi} - \dot{\tilde{\chi}} \right) = \tilde{\chi}^{T} \left(-\frac{\pi}{2p_{1}T_{1}} \left(\operatorname{sig}^{1-p_{1}} (\tilde{\chi}) + 3^{\frac{p_{1}}{2}} \operatorname{sig}^{1+p_{1}} (\tilde{\chi}) \right) - a \operatorname{sign} (\tilde{\chi}) \right) = \\
-\frac{\pi}{2p_{1}T_{1}} \sum_{m=1}^{3} \left(\left(\left| \tilde{\chi}_{m} \right|^{2} \right)^{\frac{2-p_{1}}{2}} + 3^{\frac{p_{1}}{2}} \left(\left| \tilde{\chi}_{m} \right|^{2} \right)^{\frac{2+p_{1}}{2}} \right) + a \sum_{m=1}^{3} \left(\left| \tilde{\chi}_{m} \right| \right)^{2} \leqslant -\frac{\pi}{2p_{1}T_{1}} \left(\left| \sum_{m=1}^{3} \left| \tilde{\chi}_{m} \right|^{2} \right)^{\frac{2-p_{1}}{2}} + \left(\sum_{m=1}^{3} \left| \tilde{\chi}_{m} \right|^{2} \right)^{\frac{2-p_{1}}{2}} + a \sum_{m=1}^{3} \left| \tilde{\chi}_{m} \right|^{2} = -\frac{\pi}{p_{1}T_{1}\sqrt{\lambda_{1}\lambda_{2}}} \left(\lambda_{1}V_{\chi}^{1-\frac{p_{1}}{2}} + \lambda_{2}V_{\chi}^{1+\frac{p_{1}}{2}} \right) + \rho_{1} \tag{17}$$

where $\lambda_1 = 2^{\frac{2-\rho_1}{2}}$, $\lambda_2 = 2^{\frac{2+\rho_1}{2}}$, $\rho_1 = a \sum_{m=1}^{3} |\tilde{\chi}_m|^2$.

Based on the above results, it can be concluded by Lemma 1 that $\hat{\chi}$ converges to χ in a predefined time T_1 . The proof of this theorem is completed.

2. 2 Predefined-time disturbance observer

Consider the uncertainty of inertia moment ΔJ , the dynamics of Eq.(9) can be transformed into

$$\dot{\tilde{\boldsymbol{\omega}}} = J_{0}^{-1} \Big(-(\tilde{\boldsymbol{\omega}} + \tilde{R}^{\mathsf{T}} \boldsymbol{\omega}_{\mathsf{d}}) J_{0} (\tilde{\boldsymbol{\omega}} + \tilde{R}^{\mathsf{T}} \boldsymbol{\omega}_{\mathsf{d}}) + \\ J_{0} (\tilde{\boldsymbol{\omega}}^{\mathsf{X}} \tilde{R}^{\mathsf{T}} \dot{\boldsymbol{\omega}}_{\mathsf{d}} - \tilde{R}^{\mathsf{T}} \boldsymbol{\omega}_{\mathsf{d}}) - (\tilde{\boldsymbol{\omega}} + \tilde{R}^{\mathsf{T}} \boldsymbol{\omega}_{\mathsf{d}}) \times \\ \Delta J (\tilde{\boldsymbol{\omega}} + \tilde{R}^{\mathsf{T}} \boldsymbol{\omega}_{\mathsf{d}}) + \Delta J (\tilde{\boldsymbol{\omega}}^{\mathsf{X}} \tilde{R}^{\mathsf{T}} \dot{\boldsymbol{\omega}}_{\mathsf{d}} - \tilde{R}^{\mathsf{T}} \boldsymbol{\omega}_{\mathsf{d}}) + \\ \Delta J J^{-1} (\tilde{\boldsymbol{\omega}} + \tilde{R}^{\mathsf{T}} \boldsymbol{\omega}_{\mathsf{d}})^{\mathsf{X}} J (\tilde{\boldsymbol{\omega}} + \tilde{R}^{\mathsf{T}} \boldsymbol{\omega}_{\mathsf{d}}) + \\ (I - \Delta J J^{-1}) G - \Delta J J^{-1} J (\tilde{\boldsymbol{\omega}}^{\mathsf{X}} \tilde{R}^{\mathsf{T}} \boldsymbol{\omega}_{\mathsf{d}} - \tilde{R}^{\mathsf{T}} \dot{\boldsymbol{\omega}}_{\mathsf{d}}) + \\ \boldsymbol{u} \Big) = F_{1} + G_{1} + J_{0}^{-1} \boldsymbol{u}$$

$$(18)$$

where

$$\begin{split} F_1 &= J_0^{-1} (\; -(\tilde{\boldsymbol{\omega}} + \tilde{\boldsymbol{R}}^{\mathrm{T}} \boldsymbol{\omega}_{\mathrm{d}}) J_0 (\; \tilde{\boldsymbol{\omega}} + \tilde{\boldsymbol{R}}^{\mathrm{T}} \boldsymbol{\omega}_{\mathrm{d}}) + \\ J_0 (\; \tilde{\boldsymbol{\omega}}^{\times} \tilde{\boldsymbol{R}}^{\mathrm{T}} \dot{\boldsymbol{\omega}}_{\mathrm{d}} - \tilde{\boldsymbol{R}}^{\mathrm{T}} \boldsymbol{\omega}_{\mathrm{d}})) \\ G_1 &= J_0^{-1} \Big(-(\; \tilde{\boldsymbol{\omega}} + \tilde{\boldsymbol{R}}^{\mathrm{T}} \boldsymbol{\omega}_{\mathrm{d}})^{\times} \Delta J (\; \tilde{\boldsymbol{\omega}} + \tilde{\boldsymbol{R}}^{\mathrm{T}} \boldsymbol{\omega}_{\mathrm{d}}) + \\ \Delta J (\; \tilde{\boldsymbol{\omega}}^{\times} \tilde{\boldsymbol{R}}^{\mathrm{T}} \dot{\boldsymbol{\omega}}_{\mathrm{d}} - \tilde{\boldsymbol{R}}^{\mathrm{T}} \boldsymbol{\omega}_{\mathrm{d}}) + \Delta J J^{-1} (\; \tilde{\boldsymbol{\omega}} + \tilde{\boldsymbol{R}}^{\mathrm{T}} \boldsymbol{\omega}_{\mathrm{d}})^{\times} \bullet \\ J (\; \tilde{\boldsymbol{\omega}} + \tilde{\boldsymbol{R}}^{\mathrm{T}} \boldsymbol{\omega}_{\mathrm{d}}) - \Delta J J^{-1} J (\; \tilde{\boldsymbol{\omega}}^{\times} \tilde{\boldsymbol{R}}^{\mathrm{T}} \boldsymbol{\omega}_{\mathrm{d}} - \tilde{\boldsymbol{R}}^{\mathrm{T}} \dot{\boldsymbol{\omega}}_{\mathrm{d}}) + \\ (I - \Delta J J^{-1}) (\; \tilde{\boldsymbol{\omega}}^{\times} \boldsymbol{\delta}^{\mathrm{T}} \dot{\boldsymbol{\eta}} - (\; \tilde{\boldsymbol{R}}^{\mathrm{T}} \dot{\boldsymbol{\omega}}_{\mathrm{d}})^{\times} \boldsymbol{\delta}^{\mathrm{T}} \dot{\boldsymbol{\eta}} - \boldsymbol{\delta}^{\mathrm{T}} \dot{\boldsymbol{\eta}} + d) \Big) \end{split}$$

The term G_1 can be calculated by estimating

the modal variables $\hat{\eta}$ using the proposed observer (Eq.(16)), and thus, it can be rewritten as

$$egin{aligned} ar{G}_1 &= J_0^{-1} \Big(- (\, ilde{oldsymbol{\omega}} + ilde{oldsymbol{R}}^{ op} oldsymbol{\omega}_d)^{ imes} \Delta J (\, ilde{oldsymbol{\omega}} + ilde{oldsymbol{R}}^{ op} oldsymbol{\omega}_d) + \\ & \Delta J (\, ilde{oldsymbol{\omega}}^{ imes} ilde{oldsymbol{R}}^{ op} oldsymbol{\omega}_d - ilde{oldsymbol{R}}^{ op} oldsymbol{\omega}_d) + \Delta J J^{-1} (\, ilde{oldsymbol{\omega}} + ilde{oldsymbol{R}}^{ op} oldsymbol{\omega}_d) - \Delta J J^{-1} J (\, ilde{oldsymbol{\omega}}^{ imes} ilde{oldsymbol{R}}^{ op} oldsymbol{\omega}_d - ilde{oldsymbol{R}}^{ op} oldsymbol{\dot{\omega}}_d) + \\ & (\, I - \Delta J J^{-1}) \left(\, ilde{oldsymbol{\omega}}^{ imes} oldsymbol{\delta}^{ op} \, \dot{oldsymbol{\eta}} - (\, ilde{oldsymbol{R}}^{ op} \, \dot{oldsymbol{\omega}}_d)^{ imes} oldsymbol{\delta}^{ op} \, \dot{oldsymbol{\eta}} - \\ & \delta^{ op} \, \dot{oldsymbol{\eta}} + d \, \Big) \Big) \end{aligned}$$

The system of Eq.(18) is rewritten as

$$\dot{\tilde{\boldsymbol{\omega}}} = -b_1 \tilde{\boldsymbol{\omega}} + F_1 + N + J_0^{-1} \boldsymbol{u} \tag{19}$$

where $N = b_1 \tilde{\omega} + \bar{G}_1, b_1 > 0$. For system of Eq. (19), the following auxiliary system is defined

$$\dot{x} = -b_1 x + F_1 + J_0^{-1} u \tag{20}$$

Define the discrepancy between $\tilde{\boldsymbol{\omega}}$ and x by

$$z = \tilde{\boldsymbol{\omega}} - x \tag{21}$$

Then, the error dynamics can be expressed as

$$\dot{\mathbf{z}} = \dot{\tilde{\boldsymbol{\omega}}} - \dot{\mathbf{x}} = -b_1 \mathbf{z} + \mathbf{N} \tag{22}$$

Inspired by Ref. [23], the estimation raw of the lumped disturbance is designed as

$$\hat{\bar{G}}_1 = \hat{N} - b_1 \tilde{\boldsymbol{\omega}} \tag{23}$$

where $\hat{N} = b_1 \hat{z} + \dot{z}$, and \hat{z} represents the estimation of z.

Therefore, the estimated error of the lumped disturbance is

$$\tilde{G}_{1} = \bar{G}_{1} - \hat{\bar{G}}_{1} = N - b_{1}\tilde{\omega} - (\hat{N} - b_{1}\tilde{\omega}) = N - b_{1}\hat{z} - \dot{z} = N - b_{1}\hat{z} + b_{1}z - N = b_{1}(z - \hat{z})$$
(24)

A nonlinear predefined-time observer is constructed as

$$\dot{\hat{z}} = -b_2 b_3 \tilde{z} + \dot{z} + \frac{\pi}{2p_2 T_2} \left(3^{\frac{p_z}{2}} \operatorname{sig}^{1+p_z}(\tilde{z}) + \operatorname{sig}^{1-p_z}(\tilde{z}) \right) - c \operatorname{sign}(\tilde{z})$$
(25)

where $b_2 > 0$, $b_3 > 0$, $0 < p_2 < 1$, c > 0, $\tilde{z} = z - \hat{z}$, $T_2 > 0$ is the upper bound on the convergence time of the error \tilde{z} .

Construct a Lyapunov function as

$$V_z = \frac{1}{2} \mathbf{z}^{\mathsf{T}} \mathbf{z} \tag{26}$$

Similarly, we can prove that

$$\dot{V}_{z} \leqslant -\frac{\pi}{p_{2}T_{2}\sqrt{\lambda_{3}\lambda_{4}}} \left(\lambda_{3}V_{z}^{1-\frac{\rho_{z}}{2}} + \lambda_{4}V_{z}^{1+\frac{\rho_{z}}{2}}\right) + \rho_{2}$$
(27)

where
$$\lambda_3 = 2^{\frac{2-\rho_2}{2}}$$
, $\lambda_4 = 2^{\frac{2+\rho_2}{2}}$, $\rho_2 = a \sum_{m=1}^{3} |\tilde{z}_m|^2$.

Based on the above results, it can be concluded by Lemma 1 that \hat{z} converges to z in a predefined time T_2 . The proof of this theorem is completed. Therefore, it is inferred that \hat{G}_1 is reconstructed by \hat{G}_1 after T_2 .

3 Guaranteed Performance Controller Design

3.1 Controller design

Consider a predefined performance function $\rho(t)$ proposed in Ref.[24].

$$\begin{cases}
\rho(0) = \rho_0 \\
\dot{\rho}(t) = -\mu |\rho(t) - \rho_T|^{\gamma} \operatorname{sign}(\rho(t) - \rho_T)
\end{cases}$$
(28)

where $\mu = (\rho(t) - \rho_T)^{1-\gamma}/(1-\gamma)/T_e$, T_e is the convergence time of the system states which can be predefined, γ is a constant and $\gamma \in (0,1)$, ρ_0 is the initial value of the performance function $\rho(t)$, and ρ_T is the final value of $\rho(t)$, and it satisfies

$$\rho(t) = \rho_T \quad \forall t \geqslant T_e$$

In order to stabilize the system (Eq.(18)), an virtual error angular velocity is designed as

$$\boldsymbol{\omega}^* = \boldsymbol{E}^{-1} \left[-\sigma_1 \boldsymbol{e}_{\tilde{R}} - 2\sigma_1 \frac{\rho_1^2}{\pi} \boldsymbol{\varphi}_1 \tan\left(\frac{\pi \boldsymbol{e}_{\tilde{R}}^T \boldsymbol{e}_{\tilde{R}}}{2\rho_1^2}\right) - \frac{\pi}{p T_e \sqrt{k_1 k_2}} \boldsymbol{\varphi}_1 \left(k_1 \left(\frac{\rho_1^2}{\pi} \tan\left(\frac{\pi \boldsymbol{e}_{\tilde{R}}^T \boldsymbol{e}_{\tilde{R}}}{2\rho_1^2}\right)\right)^{1 - \frac{P}{2}} + k_2 2^{\frac{P}{2}} \left(\frac{\rho_1^2}{\pi} \tan\left(\frac{\pi \boldsymbol{e}_{\tilde{R}}^T \boldsymbol{e}_{\tilde{R}}}{2\rho_1^2}\right)\right)^{1 + \frac{P}{2}} \right) \right]$$

$$(29)$$

where
$$v_1 = e_{ar{R}}/\cos^2\!\!\left(rac{\pi e_{ar{R}}^{\mathrm{T}}e_{ar{R}}}{2
ho_1^2}
ight)$$
, $\sigma_1 = \sqrt{\left(rac{\dot{
ho}_1}{
ho_1}
ight)^2 + \Delta_1}$, ho_1

is the performance function to constrain the tracking error $e_{\bar{R}}$, Δ_1 is a small positive constant, φ_1 =

$$\frac{\boldsymbol{e}_{\tilde{R}}}{\left\|\boldsymbol{e}_{\tilde{R}}\right\|^{2}}\cos^{2}\!\!\left(\frac{\boldsymbol{\pi}\boldsymbol{e}_{\tilde{R}}^{\mathrm{T}}\boldsymbol{e}_{\tilde{R}}}{2\rho_{1}^{2}}\right)\!\!,\;k_{1}\!>\!0,k_{2}\!>\!0,\;\mathrm{and}\;0\!<\!p\!<\!1.$$

Denote ω_e as the error between the error angular velocity and the virtual error angular velocity, that is

$$\boldsymbol{\omega}_{e} = \tilde{\boldsymbol{\omega}} - \boldsymbol{\omega}^{*} \tag{30}$$

Then, based on the estimation results of the introduced observer (Eq.(25)), the following predefined-time controller can be designed for the attitude error system.

$$\boldsymbol{u} = -\boldsymbol{J}_{0} \left[\boldsymbol{F}_{1} + \hat{\boldsymbol{G}}_{1} - \boldsymbol{\dot{\omega}}^{*} + \cos^{2} \left(\frac{\boldsymbol{\pi} \boldsymbol{\omega}_{e}^{T} \boldsymbol{\omega}_{e}}{2\rho_{2}^{2}} \right) \boldsymbol{E} \boldsymbol{v}_{1} + \right]$$

$$2\sigma_{2} \frac{\rho_{2}^{2}}{\boldsymbol{\pi}} \boldsymbol{\varphi}_{2} \tan \left(\frac{\boldsymbol{\pi} \boldsymbol{\omega}_{e}^{T} \boldsymbol{\omega}_{e}}{2\rho_{2}^{2}} \right) + \left[\frac{\boldsymbol{\pi}}{p T_{e} \sqrt{k_{1} k_{2}}} \boldsymbol{\varphi}_{2} \left(k_{1} \left(\frac{\rho_{1}^{2}}{\boldsymbol{\pi}} \tan \left(\frac{\boldsymbol{\pi} \boldsymbol{\omega}_{e}^{T} \boldsymbol{\omega}_{e}}{2\rho_{2}^{2}} \right) \right)^{1 - \frac{\rho}{2}} + \right]$$

$$k_{2} \frac{\rho_{2}^{P}}{2} \left(\frac{\rho_{1}^{2}}{\boldsymbol{\pi}} \tan \left(\frac{\boldsymbol{\pi} \boldsymbol{\omega}_{e}^{T} \boldsymbol{\omega}_{e}}{2\rho_{2}^{2}} \right) \right)^{1 + \frac{\rho}{2}} \right) - \frac{h^{2}}{2} \boldsymbol{v}_{2}$$

$$(31)$$

where
$$v_2 = \boldsymbol{\omega}_e / \cos^2 \left(\frac{\pi \boldsymbol{\omega}_e^{\mathrm{T}} \boldsymbol{\omega}_e}{2\rho_2^2} \right)$$
, $\sigma_2 = \sqrt{\left(\frac{\dot{\rho}_2}{\rho_2} \right)^2 + \Delta_2}$,

 ρ_2 is the performance function to constrain the tracking error $\boldsymbol{\omega}_e$, Δ_2 is a small positive constant, $\boldsymbol{\varphi}_2$ =

$$\frac{\boldsymbol{\omega}_{\epsilon}}{\|\boldsymbol{\omega}_{\epsilon}\|^2}\cos^2\!\left(\frac{\pi\boldsymbol{\omega}_{\epsilon}^{\mathrm{T}}\boldsymbol{\omega}_{\epsilon}}{2\rho_2^2}\right)$$
, and $h > 0$.

3. 2 Stability analysis

Define the tan-type BLF as

$$V_{1} = \frac{\rho_{1}^{2}}{\pi} \tan \left(\frac{\pi e_{\tilde{R}}^{\mathrm{T}} e_{\tilde{R}}}{2\rho_{1}^{2}} \right) \tag{32}$$

The time-derivative of the BLF is obtained as

$$\dot{V}_{1} = \frac{2\rho_{1}\dot{\rho}_{1}}{\pi} \tan\left(\frac{\pi e_{\tilde{R}}^{\mathsf{T}} e_{\tilde{R}}}{2\rho_{1}^{2}}\right) - \frac{\dot{\rho}_{1}}{\rho_{1}} \frac{e_{\tilde{R}}^{\mathsf{T}} e_{\tilde{R}}}{\cos^{2}\left(\frac{\pi e_{\tilde{R}}^{\mathsf{T}} e_{\tilde{R}}}{2\rho_{1}^{2}}\right)} + \frac{e_{\tilde{R}}^{\mathsf{T}} e_{\tilde{R}}}{\cos^{2}\left(\frac{\pi e_{\tilde{R}}^{\mathsf{T}} e_{\tilde{R}}}{2\rho_{1}^{2}}\right)} \dot{e}_{\tilde{R}} \leq 2\sigma_{1}\frac{\rho_{1}^{2}}{\pi} \tan\left(\frac{\pi e_{\tilde{R}}^{\mathsf{T}} e_{\tilde{R}}}{2\rho_{1}^{2}}\right) + \sigma_{1}v_{1}^{\mathsf{T}} e_{\tilde{R}} + v_{1}^{\mathsf{T}} \dot{e}_{\tilde{R}} = 2\sigma_{1}\frac{\rho_{1}^{2}}{\pi} \tan\left(\frac{\pi e_{\tilde{R}}^{\mathsf{T}} e_{\tilde{R}}}{2\rho_{1}^{2}}\right) + \sigma_{1}v_{1}^{\mathsf{T}} e_{\tilde{R}} + v_{1}^{\mathsf{T}} E\left(\boldsymbol{\omega}_{e} + \boldsymbol{\omega}^{*}\right) = v_{1}^{\mathsf{T}} E\boldsymbol{\omega}_{e} - \frac{\pi}{pT_{e}\sqrt{k_{1}k_{2}}} \left(k_{1}V_{1}^{1-\frac{\tilde{p}}{2}} + k_{2}2^{\frac{\tilde{p}}{2}}V_{1}^{1+\frac{\tilde{p}}{2}}\right)$$

$$(33)$$

Another BLF is considered as

$$V_2 = \frac{\rho_2^2}{\pi} \tan \left(\frac{\pi e_{\hat{R}}^{\mathrm{T}} e_{\hat{R}}}{2\rho_2^2} \right) \tag{34}$$

The time derivative of V_2 can be written as follows

$$\dot{V}_{2} = \frac{2\rho_{2}\dot{\rho}_{2}}{\pi} \tan\left(\frac{\pi\boldsymbol{\omega}_{e}^{T}\boldsymbol{\omega}_{e}}{2\rho_{2}^{2}}\right) - \frac{\dot{\rho}_{2}}{\rho_{2}} \frac{\boldsymbol{\omega}_{e}^{T}\boldsymbol{\omega}_{e}}{\cos^{2}\left(\frac{\pi\boldsymbol{\omega}_{e}^{T}\boldsymbol{\omega}_{e}}{2\rho_{2}^{2}}\right)} + \frac{\boldsymbol{\omega}_{e}^{T}}{\cos^{2}\left(\frac{\pi\boldsymbol{\omega}_{e}^{T}\boldsymbol{\omega}_{e}}{2\rho_{2}^{2}}\right)} \dot{\boldsymbol{\omega}}_{e} \leq 2\sigma_{2}\frac{\rho_{2}^{2}}{\pi} \tan\left(\frac{\pi\boldsymbol{\omega}_{e}^{T}\boldsymbol{\omega}_{e}}{2\rho_{2}^{2}}\right) + \sigma_{2}\boldsymbol{v}_{2}^{T}\boldsymbol{\omega}_{e} + \boldsymbol{v}_{2}^{T}\dot{\boldsymbol{\omega}}_{e} = 2\sigma_{2}\frac{\rho_{2}^{2}}{\pi} \tan\left(\frac{\pi\boldsymbol{\omega}_{e}^{T}\boldsymbol{\omega}_{e}}{2\rho_{2}^{2}}\right) + \sigma_{2}\boldsymbol{v}_{2}^{T}\boldsymbol{\omega}_{e} + \boldsymbol{v}_{2}^{T}(\boldsymbol{F}_{1} + \boldsymbol{\bar{G}}_{1} + \boldsymbol{J}_{0}^{-1}\boldsymbol{u} - \dot{\boldsymbol{\omega}}^{*}) = -\boldsymbol{\omega}_{e}^{T}\boldsymbol{E}\boldsymbol{v}_{1} + \boldsymbol{v}_{2}^{T}(\boldsymbol{\bar{G}}_{1} - \hat{\boldsymbol{G}}_{1}) + \frac{h^{2}}{2}\boldsymbol{v}_{2}^{T}\boldsymbol{v}_{2} - \frac{\pi}{\rho T_{e}\sqrt{k_{1}k_{2}}}\left(k_{1}\boldsymbol{V}_{2}^{1-\frac{\rho}{2}} + k_{2}2^{\frac{\rho}{2}}\boldsymbol{V}_{2}^{1+\frac{\rho}{2}}\right) \tag{35}$$

It is worth noting that $e = \bar{G}_1 - \hat{\bar{G}}_1 = 0$ is obtained for $T \geqslant T_2$.

Define
$$V = V_1 + V_2$$
, and it can be derived that $\dot{V} = \dot{V}_1 + \dot{V}_2 \leqslant -\frac{\pi}{pT_e\sqrt{k_1k_2}} \left(k_1 \left(V_1^{1-\frac{p}{2}} + V_2^{1-\frac{p}{2}}\right) + k_2 2^{\frac{p}{2}} \left(V_1^{1+\frac{p}{2}} + V_2^{1+\frac{p}{2}}\right)\right) + \frac{1}{2h^2} \|\mathbf{v}_2\|^2$ (36)

It can be derived by Lemma 2 that

$$egin{align*} V_1^{1-rac{ heta}{2}} + V_2^{1-rac{ heta}{2}} &\geqslant & (V_1 + V_2)^{1-rac{ heta}{2}} \ V_1^{1+rac{ heta}{2}} + V_2^{1+rac{ heta}{2}} &\geqslant & 2^{-rac{ heta}{2}} (V_1 + V_2)^{1+rac{ heta}{2}} \end{aligned}$$

With the above relations, it can be obtained from Eq.(36) that

$$\dot{V} \leqslant -\frac{\pi}{\rho T_e \sqrt{k_1 k_2}} \left(k_1 V^{1 - \frac{\rho}{2}} + k_2 V^{1 + \frac{\rho}{2}} \right) + \rho_3 \qquad (37)$$

where $\rho_3 = \frac{h^2}{2} \| \mathbf{v}_2 \|^2$. According to Lemma 1, it can be proved that the BLF V will converge to a bounded domain within predefined-time. According to the property of BLF, $\| \mathbf{e}_{\tilde{R}} \| \leq \rho_1(t)$, $\| \mathbf{w}_e \| \leq \rho_2(t)$ always exist. Therefore, the prescribed performance functions $\rho_1(T_e)$ constraints $\mathbf{e}_{\tilde{R}}$ and $\rho_2(T_e)$ constraints \mathbf{w}_e after T_e . Thus, the virtual error angular velocity \mathbf{w}^* approaches 0, from which we can obtain that the spacecraft's angular velocity error $\tilde{\mathbf{w}} \to 0$ within T_e .

4 Simulation Results

To verify the effectiveness of the proposed predefined-time controller, numerical simulations for a flexible spacecraft are conducted in two cases, and the sampling time is 0.01 s. A set of comparative simulation experiments with Ref.[25] of finite-time attitude tracking controller (FTATC) are carried out to reflect the superiority of the proposed control algorithm in terms of settling time, convergence accuracy and fault-tolerant performance. A flexible spacecraft^[26] characterized by a nominal inertia matrix J_0 =[22,0.3,-0.4;0.3,23,0.3;-0.4,0.3,24] kg·m² and a uncertain inertia matrix ΔJ =0.1J is considered, respectively. The initial states are presented as

$$R(0) = \begin{bmatrix} 0.2887 & 0.4802 & -0.8660 \\ -0.8165 & 0.5774 & 0 \\ 0.5000 & 0.0701 & 0.5000 \end{bmatrix}$$
$$\eta(0) = \begin{bmatrix} 0 & 0 & 0 & 0 \end{bmatrix}^{T}$$
$$\dot{\eta}(0) = \begin{bmatrix} 0 & 0 & 0 & 0 \end{bmatrix}^{T}$$
$$\omega(0) = \begin{bmatrix} 0 & 0 & 0 & 0 \end{bmatrix}^{T}$$

Moreover, the damping ratio, the natural frequency and the coupling matrix are respectively computed as

 $\xi_1 = 0.056, \xi_2 = 0.086, \xi_3 = 0.08, \xi_4 = 0.02, l_1 = 1.0793, l_2 = 1.2761, l_3 = 1.6358, l_4 = 2.2893$

$$\boldsymbol{\delta} = \begin{bmatrix} 1.3525 & 1.2784 & 2.1530 \\ -1.1519 & 1.0176 & -1.224 \\ 2.2167 & 1.5891 & -0.8324 \\ 1.2367 & -1.6537 & 0.2251 \end{bmatrix}$$

The disturbances are set as

$$d(t) = [\sin(0.1t), \cos(0.2t), \sin(0.2t)]^{T} \text{ N} \cdot \text{m}$$

The desired attitude and angular velocity are respectively

$$R_{\rm d}(0) = I$$

 $\omega_{\rm d} = 0.05 [\sin(\pi t/100), -\cos(2\pi t/100), \sin(3\pi t/100)]^{\rm T} \text{ rad/s}$

The parameters of the prescribed performance function are set as $\rho(0) = 0.7$, $\gamma = 0.15$, $T_e = 20$, the final value of $\mathbf{e}_{\tilde{\mathbf{k}}}$ is $\rho_1(t) = 0.01$, and the final value of $\mathbf{\omega}_e$ is $\rho_2(t) = 0.005$. The virtual estimation error of $\mathbf{\omega}_e$ is limited by ρ_2 and the attitude error $\mathbf{e}_{\tilde{\mathbf{k}}}$ is limited by ρ_1 . Therefore, $\rho_1(0) > \|\mathbf{e}_{\tilde{\mathbf{k}}}(0)\|$, $\rho_2(0) > \|\mathbf{\omega}_e(0)\|$. And the setting of T_e affects the slope of $\rho(t)$, which exerts an influence on the changing trend of $\mathbf{e}_{\tilde{\mathbf{k}}}$ and $\mathbf{\omega}_e$. Besides, $\rho_1(T_e)$, $\rho_2(T_e)$ determine the steady-state errors of $\|\mathbf{e}_{\tilde{\mathbf{k}}}\|$, $\|\mathbf{\omega}_e\|$.

In addition, the parameters of the predefined time observers are appointed as $p_1 = 0.15$, $T_1 =$ $T_2 = 10, c = 0.01, b_1 =$ $5, a = 0.01, p_2 = 0.005,$ 0.95, $b_2 = 0.2$, $b_3 = 0.2$. To design the disturbance observer (Eq.(25)), it is necessary to obtain the estimations of flexible modes through the modal observer(Eq.(15)). Therefore, the relationship of the two parameters T_1 and T_2 is $T_1 < T_2$. Besides, the setting of T_1 and T_2 can impact the convergence time of the two observers. And the other parameters can be adjusted through a trial-and-error method. What's more, the impact of parameters on the observer's performance is tested by observing the estimation errors of η and G_1 , and the following controller parameters have no effect on the observer's results.

The parameters related to the predefined-time prescribed performance controller (PTPPC) are p = 0.9, $k_1 = 0.2$, $k_2 = 0.2$, $T_e = 20$. The designing of controller (Eq.(31)) is based on an ideal esti-

mation effect of the above observers, which is the reason for $T_e > T_1$, $T_e > T_2$.

The high-accuracy of the proposed controller is observed by selecting the variation curves of the tracking errors. The simulation results of this paper are compared with those of the finite-time controller (FTC) in Ref.[25], and the initial conditions and flexible spacecraft model are the same for both. Assuming the attitude errors are less than 5×10^{-4} that reaches the stable accuracy. Fig.3 reflects the results of the attitude tracking of PTPPC, from which it can be seen that the attitude tracking errors converge to equilibrium within 18 s. Fig.4 shows that with the simulation results of FTC designed in Ref.[25], the attitude errors converge to 5×10^{-4} after 30 s, and fluctuations occur in attitude tracking process during subsequent.

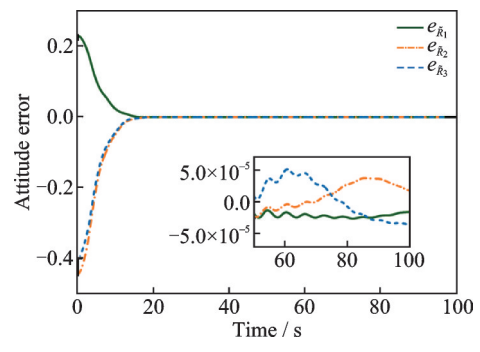


Fig. 3 Response curves of attitude tracking errors $e_{\vec{k}}$ of PTPPC

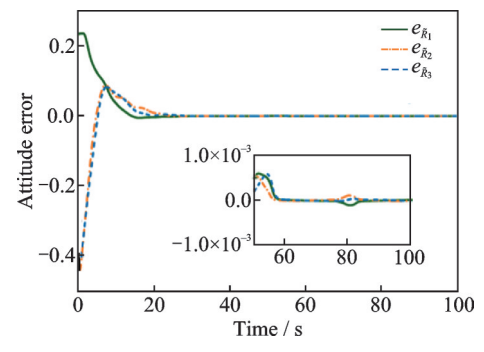


Fig.4 Response curves of attitude tracking errors $e_{\tilde{R}}$ of FTC

Fig.5 shows the spacecraft's angular velocity curves, from which it can be seen that the angular velocity errors of PTPPC converge to the equilibrium at 18.5 s and the accuracy can reach 5×10^{-5} , while FTC needs 30.5 s in Fig.6. Moreover, supposing that the final values of angular velocity errors in simulations represent attitude control accuracy,

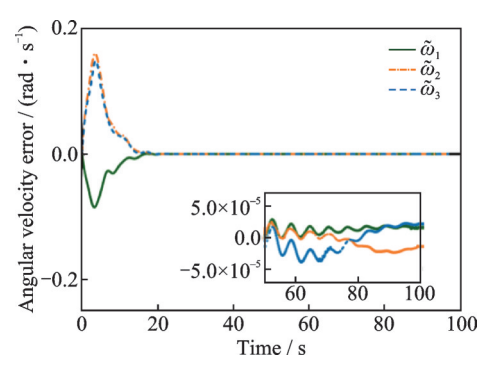


Fig. 5 Response curves of angular velocity tracking errors $\tilde{\pmb{\omega}}$ of PTPPC

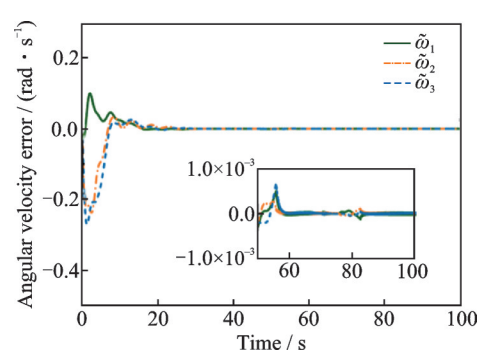


Fig. 6 Response curves of angular velocity tracking errors $\tilde{\omega}$ of FTC

the final attitude stability of PTPPC is much higher than that of FTC.

In addition, Fig.7 illustrates the control torque of the flexible spacecraft, from which it can be seen that the maximum torque is 1.6 N·m of the actuator. The PTPPC has much smaller maximum than that of FTC (Fig.8), meaning it is more suitable for practical applications. As the spacecraft approaches the desired attitude, the control torques gradually decrease.

The flexible vibrations are represented in Fig.9, it is seen that the flexible vibrations are bounded. The estimation performance of the observer is shown in Fig.10 and Fig.11. From Fig.12 and

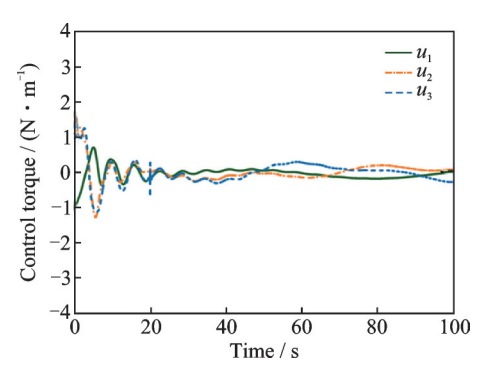


Fig. 7 Response curves of control torque u of PTPPC

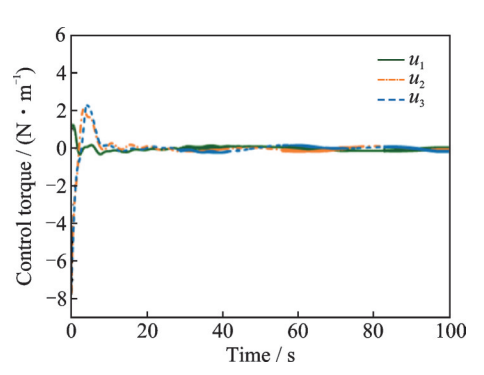


Fig. 8 Response curves of control torque u of FTC

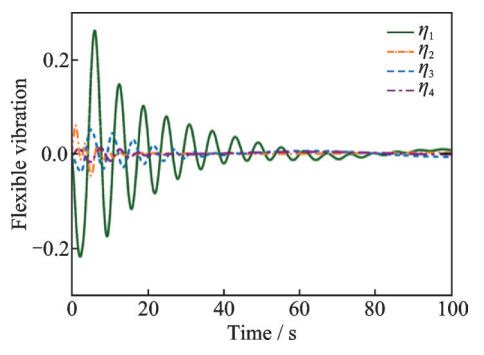


Fig. 9 Response curves of flexible vibration η of PTPPC

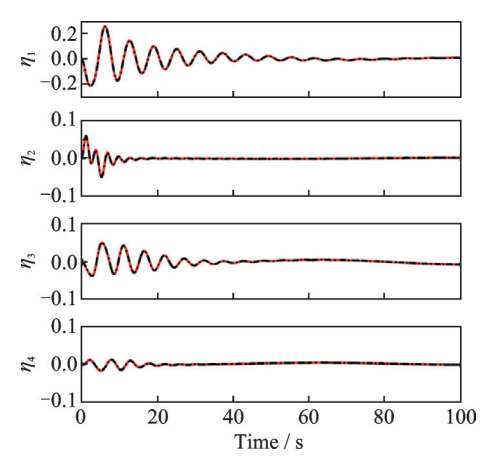


Fig. 10 The estimation of η of PTPPC

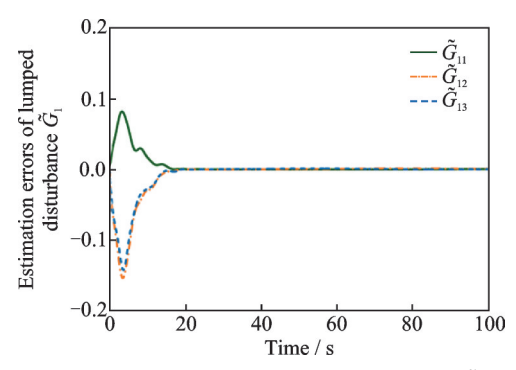


Fig.11 Estimation errors of lumped disturbance \tilde{G}_1 of PTPPC

Fig.13, it can be seen that the $\|e_{\tilde{R}}\|$ and $\|\omega_e\|$ consistently satisfy the constraints of the performance function.

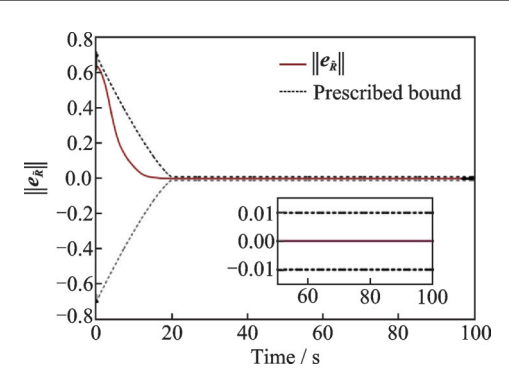


Fig.12 Response curves of $\|e_{\tilde{R}}\|$ of PTPPC

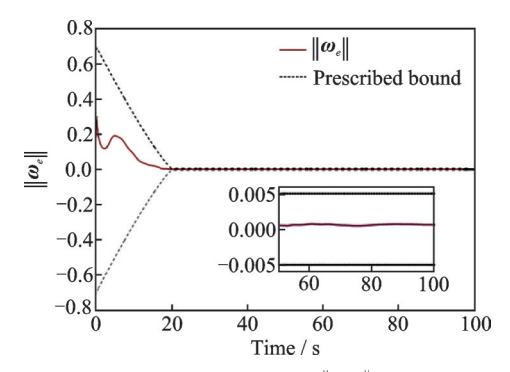


Fig.13 Response curves of $\|\boldsymbol{\omega}_e\|$ of PTPPC

To sum up, the proposed PTPPC has faster transient response and higher convergence quality compared with those of FTC. Thus, the practicality and superiority of the controller designed in this paper are verified.

5 Conclusions

For the attitude tracking problem in the attitude tracking process of flexible spacecraft, a predefined-time guaranteed performance controller based on multi-observer is proposed. The convergence time of the system can be predefined, which is not affected by the initial conditions. Moreover, the designed controller is capable to handle multiple disturbances to achieve robustness. The superiority of the proposed controller is validated compared with that of the finite-time controller. The higher control precision, faster convergence rate, and smaller control inputs are all achieved.

References

[1] YANG Y X, CHEN M, PENG K X, et al. Adaptive sliding mode fault-tolerant control for attitude tracking of spacecraft with actuator faults[J]. International Journal of Control, Automation and Systems, 2023,

- 21(8): 2587-2594.
- [2] SANWALE J, SALAHUDDEN S, GIRI D K. Neuro-adaptive fault-tolerant sliding mode controller for spacecraft attitude stabilization[J]. Journal of Spacecraft and Rockets, 2021, 58(6): 1924-1929.
- [3] WANG J, HU Y S, JI W Q. Barrier function-based adaptive integral sliding mode finite-time attitude control for rigid spacecraft[J]. Nonlinear Dynamics, 2022, 110(2): 1405-1420.
- [4] PESCE V, SILVESTRINI S, LAVAGNA M. Radial basis function neural network aided adaptive extended Kalman filter for spacecraft relative navigation[J]. Aerospace Science and Technology, 2020, 96: 105527.
- [5] SHARMA S, D'AMICO S. Neural network-based pose estimation for noncooperative spacecraft rendezvous[J]. IEEE Transactions on Aerospace and Electronic Systems, 2020, 56(6): 4638-4658.
- [6] AZIMI M, SHARIFI G. A hybrid control scheme for attitude and vibration suppression of a flexible spacecraft using energy-based actuators switching mechanism[J]. Aerospace Science and Technology, 2018, 82: 140-148.
- [7] LIU Y, ZHANG H, ZHANG S, et al. Minimum-learning-parameter-based fault-tolerant control for spacecraft rendezvous with unknown inertial parameters[J]. IEEE Access, 2020, 8: 151487-151499.
- [8] GIRI D K, SINHA M. Robust backstepping magnetic attitude control of satellite subject to unsymmetrical mass properties[J]. Journal of Spacecraft and Rockets, 2019, 56(1): 298-305.
- [9] HU Q L, XIAO L, WANG C L. Adaptive fault-tolerant attitude tracking control for spacecraft with time-varying inertia uncertainties[J]. Chinese Journal of Aeronautics, 2019, 32(3): 674-687.
- [10] LEE T. Exponential stability of an attitude tracking control system on SO(3) for large-angle rotational maneuvers[J]. Systems & Control Letters, 2012, 61 (1): 231-237.
- [11] MA J J, LI P. Finite-time attitude stabilization of an output-constrained rigid spacecraft[J]. International Journal of Advanced Robotic Systems, 2020, 17: 1729881420907416.
- [12] GAO S H, LIU X P, JING Y W, et al. Finite-time prescribed performance control for spacecraft attitude tracking[J]. IEEE/ASME Transactions on Mechatronics, 2022, 27(5): 3087-3098.
- [13] CHEN Q, XIE S Z, SUN M X, et al. Adaptive nonsingular fixed-time attitude stabilization of uncertain

- spacecraft[J]. IEEE Transactions on Aerospace and Electronic Systems, 2018, 54(6); 2937-2950.
- [14] WANG F, MIAO Y, LI C Y, et al. Attitude control of rigid spacecraft with predefined-time stability[J]. Journal of the Franklin Institute, 2020, 357(7): 4212-4221.
- [15] XIE S Z, CHEN Q. Adaptive nonsingular predefinedtime control for attitude stabilization of rigid spacecrafts[J]. IEEE Transactions on Circuits and Systems II: Express Briefs, 2022, 69(1): 189-193.
- [16] SAINI V K, GIRI D K, VARATHARAJOO R. Prescribed-time spacecraft attitude control using time-varying state feedback[J]. Journal of Spacecraft and Rockets, 2023, 60(4): 1242-1255.
- [17] SUN H J, WU Y Y, ZHANG J X. A distributed predefined-time attitude coordination control scheme for multiple rigid spacecraft[J]. Aerospace Science and Technology, 2023, 133: 108134.
- [18] GUO Y N, WANG P Y, MA G F, et al. Prescribed performance based finite-time attitude tracking control for rigid spacecraft[C]//Proceedings of the 2018 Eighth International Conference on Information Science and Technology (ICIST). Cordoba, Granada, and Seville, Spain: IEEE, 2018: 121-126.
- [19] HUANG HF, HEW, LIJS, et al. Disturbance observer-based fault-tolerant control for robotic systems with guaranteed prescribed performance[J]. IEEE Transactions on Cybernetics, 2022, 52(2): 772-783.
- [20] YAO Q J, LI Q, HUANG J C, et al. PDE-based prescribed performance adaptive attitude and vibration control of flexible spacecraft[J]. Aerospace Science and Technology, 2023, 141: 108504.
- [21] WU C H, YAN J G, SHEN J H, et al. Predefined-time attitude stabilization of receiver aircraft in aerial refueling[J]. IEEE Transactions on Circuits and Systems II: Express Briefs, 2021, 68(10): 3321-3325.
- [22] SUI W S, DUAN G R, HOU M Z, et al. Distributed fixed-time attitude coordinated tracking for multiple rigid spacecraft via a novel integral sliding mode approach[J]. Journal of the Franklin Institute, 2020, 357 (14): 9399-9422.
- [23] GOLESTANI M, ZHANG W D, YANG Y X, et al. Disturbance observer-based constrained attitude control for flexible spacecraft[J]. IEEE Transactions on Aerospace and Electronic Systems, 2023, 59(2): 963-972.
- [24] LUO Jianjun, WEI Caisheng, and YIN Zeyang. Pre-

- scribed performance control and its aerospace applications[M]. Beijing: National Defence Industry Press, 2023. (in Chinese)
- [25] GAO Z, ZHU Z H. Adaptive fast sliding model attitude tracking control for flexible spacecraft[C]//Proceedings of the 2018 IEEE 4th International Conference on Control Science and Systems Engineering (ICCSSE). Wuhan, China; IEEE, 2018; 264-268.
- [26] ZHAO H, WU X D, XIE Y E, et al. Rotation matrix-based finite-time attitude synchronization control for flexible spacecrafts with unknown inertial parameters and actuator faults[J]. ISA Transactions, 2022, 128: 276-289.

Acknowledgements This work was supported by the National Natural Science Foundation of China (No.12472045) and the Shanghai Aerospace Science and Technology Innovation Fund (No.SAST2022-036).

Authors

The first author Ms. DENG Xingting received her M.S. degree in control engineering from Nanjing University of Aeronautics and Astronautics, China, in 2025. She is currently working in Shanghai Engineering Center for Microsat, Shanghai, China. Her research interest is spacecraft attitude control.

The corresponding author Prof. LI Shuang received his Ph.D. degree from Harbin Institute of Technology, Harbin, China, in 2007. He works as a professor at Nanjing University of Aeronautics and Astronautics. His research interests are focused on spacecraft dynamics and control, aircraft game confrontation planning and control, and intelligent planning for multi-satellite networked collaborative observation.

Author contributions Ms. DENG Xingting formulated the research plan, carried out core experiments, simulations and analysis, and completed the writing and revision of the paper. Prof. LI Shuang offered significant recommendations regarding the paper's research ideas, methods and results. Mr. ZHANG Ziyang and Mr. WANG Beichao participated in writing and revising the initial draft of the paper. Mr. WANG Guohua and Ms. LI Fangfang engaged in literature research and collation of experimental records, and optimized the structure of the paper. All authors commented on the manuscript draft and approved the submission.

Competing interests The authors declare no competing interests.

基于多观测器的挠性航天器预设时间保证性能姿态跟踪控制

邓兴婷^{1,2},张子扬¹,王北超¹,王国华²,李芳芳²,李 爽¹ (1.南京航空航天大学航天学院,南京 211106,中国; 2.上海微小卫星工程中心,上海 201306,中国)

摘要:为解决挠性航天器在姿态跟踪过程中存在的外部环境干扰、惯性参数不确定性及挠性模态振动等问题,提出一种基于多观测器的预设时间保证性能控制器。首先,为避免姿态描述中出现退绕问题,基于旋转矩阵描述了航天器的姿态。其次,针对实际情况中挠性模态难以测量的情况,设计了能在预设时间内收敛的挠性模态观测器;此外,引入干扰观测器对集总扰动进行估计与补偿,以提高姿态控制的鲁棒性;提出了一种基于障碍 Lyapunov 函数的预设时间控制器,用于保证系统状态达到预先设定的性能并稳定姿态跟踪系统。最后,对比仿真实验结果表明,与现有的有限时间姿态跟踪控制器相比,本文的控制器能够实现更高精度的收敛。本文为存在多种扰动的挠性航天器高精度预设时间保证性能姿态跟踪提供了参考。

关键词:挠性航天器;保证性能;预设时间控制;多观测器